

## An effective search method for gravitational ringing of black holes

Hiroyuki Nakano,<sup>1</sup> Hirotaka Takahashi,<sup>2,3</sup> Hideyuki Tagoshi,<sup>3</sup> and Misao Sasaki<sup>4</sup>

<sup>1</sup>*Department of Mathematics and Physics, Graduate School of Science, Osaka City University, Osaka 558-8585, Japan*

<sup>2</sup>*Department of Physics, Graduate School of Science and Technology, Niigata University, Niigata 950-2181, Japan*

<sup>3</sup>*Department of Earth and Space Science, Graduate School of Science, Osaka University, Toyonaka, 560-0043, Japan*

<sup>4</sup>*Yukawa Institute for Theoretical Physics, Kyoto University, Kyoto 606-8502, Japan*

(Received 19 June 2003; published 21 November 2003)

We develop a search method for gravitational ringing of black holes. The gravitational ringing is due to complex frequency modes called the quasinormal modes that are excited when a black hole geometry is perturbed. The detection of it will be a direct confirmation of the existence of a black hole. Assuming that the ringdown waves are dominated by the least-damped (fundamental) mode with the least imaginary part, we consider matched filtering and develop an optimal method to search for the ringdown waves that have damped sinusoidal wave forms. When we use the matched filtering method, a data analysis with a lot of templates is required. Here we have to ensure a proper match between the filter as a template and the real wave. It is necessary to keep the detection efficiency as high as possible under limited computational costs. First, we consider the white noise case for which the matched filtering can be studied analytically. We construct an efficient method for tiling the template space. Then, using a fitting curve of the TAMA300 DT7 noise spectrum, we numerically consider the case of colored noise. We find our tiling method developed for the white noise case is still valid even if the noise is colored.

DOI: 10.1103/PhysRevD.68.102003

PACS number(s): 04.80.Nn, 07.05.Kf

### I. INTRODUCTION

There are many ongoing projects of gravitational wave detection around the world; the Laser Interferometric Gravitational Wave Observatory (LIGO) [1], VIRGO [2], GEO-600 [3], ACIGA [4] and TAMA300 [5] which are ground-based laser interferometers, and EXPLORER [6], ALLEGRO [7], NIOBE [8], NAUTILUS [9] and AURIGA [10] which are bar detectors. Furthermore, there are some future space interferometer projects such as the Laser Interferometer Space Antenna (LISA) [11].

The detection of gravitational waves provides us with not only a direct experimental test of general relativity but also a new window to observe our Universe. To use them as a new tool of observation, it is necessary to know the theoretical waveforms. Once we know them, we may appeal to the matched filtering technique to extract the source's information from gravitational wave signals. However, because the signals are expected to be very weak and the amount of data will be enormous for long-term continuous observations, it is essentially important to develop efficient data analysis methods.

For the ground-based and future space-based interferometers, the coalescences of compact object binaries are the most important sources of gravitational waves. The process of coalescence can be divided into three distinct phases. During an *inspiral* phase, the gravitational radiation reaction time scale is much longer than the orbital period. The gravitational waves from the inspiral carry the information of the masses and spins of the systems and so on. After the inspiral, compact object binaries encounter the dynamical instability and then would merge. This phase is called as a *merger* phase. The gravitational waves from the merger give us the information about the highly nonlinear dynamics of relativistic gravity. Finally, if a black hole is formed by merger, this

system can be describe as oscillations of this final black hole's quasinormal modes and then settles down to a stationary Kerr state. The emitted gravitational waves in this *ringdown* phase carry the information about the mass and spin of the final black hole.

In this paper, we consider gravitational ringing of distorted spinning (Kerr) black holes. The ringdown waves are due to quasinormal modes of black holes that are complex frequency wave solutions of the perturbed Einstein equations with purely outgoing-wave boundary condition at infinity and ingoing-wave at horizon, with vanishing incoming-wave amplitude. A quasinormal mode is characterized by the central frequency  $f_c$ , usually called the (quasi-)normal-mode frequency, and the quality factor  $Q$  which is inversely proportional to the imaginary part of the complex frequency. The gravitational waves emitted at the last stage of the formation of a black hole are also expected to be dominated by the quasinormal modes.

The quasinormal modes can be obtained by solving the Teukolsky equation that governs the perturbation of a Kerr black hole. Their properties were analyzed extensively by Leaver [12], and it is known that the least-damped mode belongs to the  $\ell = m = 2$  spin-2 spheroidal harmonic modes. The dependence of the parameters  $\{f_c, Q\}$  of the least-damped mode on the black hole parameters  $\{M, J\}$ , where  $M$  is the black hole mass and  $J$  is the spin angular momentum, is briefly reviewed in Sec. II. Assuming that the ringdown waves are dominated by the least-damped mode, the black hole parameters  $\{M, J\}$  can be uniquely determined by measuring the parameters  $\{f_c, Q\}$  of the gravitational wave signal.

It is noted that the ringdown signal decays exponentially. If the signal to noise ratio (SNR) is large, not much effort is needed to detect the signal, but if the SNR is small, the signal is going to be buried inside the noise even more after

just one wave length, and there is absolutely no hope of seeing many more cycles, specifically because the signal drops exponentially with time. So, we have to treat the loss of the SNR not to be large.

Methods to search for the ringdown waves were discussed previously by several authors. Echeverria [13] investigated the problem of extracting the black hole parameters from gravitational wave data in the case when the signal-to-noise ratio (SNR) is large. Finn [14] improved this situation by developing a maximum likelihood analysis method that can deal with any SNR. Flanagan and Hughes then considered the parameter extraction from the three stages of a binary coalescence, i.e., from inspiral, merger and ringdown phases, in their series papers [15]. For the ringdown phase, they discussed the relation between the energy spectrum of the radiation and the SNR. Creighton [16] reported the results of analyzing data of the Caltech 40m by matched filtering, and emphasized the importance of coincidence event searches to discriminate spurious events from real events. But the search was limited to a single ringdown wave template. In order to treat ringdown waves with unknown parameters, we need to prepare a lot of theoretical templates. It is necessary to keep the loss of the SNR as small as possible under limited computational costs. So, we should consider an effective template spacing. Recently, Arnaud *et al.* [17] have discussed a tiling method to cover the 2-dimensional template space  $\{f_c, Q\}$ . In this paper, we develop a different tiling method which is much more efficient than that of [17] and examine the efficiency with TAMA300 DT7 noise spectrum.

Here we make a comment on combining this search technique of ringdown waves with the current search techniques for the earlier two stages of the process in the coalescence of compact object binaries, i.e., inspiral and merger phases. Ultimately, the search method and the data analysis approach should be able to handle all the three phases in a unified manner, going smoothly from one phase to the next. In the present state, it may be difficult to obtain the parameters of the final black hole from the gravitational waves in the inspiral and merger phases. However, in the case when a compact star is inspiraling into a super massive black hole, we will be able to obtain the information about the mass of a super massive black hole from the gravitational waves in the inspiral phase. This will improve the detection efficiency of ringdown waves significantly.

The paper is organized as follows. In Sec. II, we briefly review the quasinormal modes of spinning black holes. In Sec. III, we consider the template space  $\{f_c, Q\}$  for the white noise case analytically and develop an efficient tiling method. In Sec. IV, by using a fitting curve for the TAMA DT7 noise spectrum, we show that our tiling method developed in the case of white noise is valid even in the case of colored noise. Section V is devoted to summary and discussion. In Appendix A, we discuss simpler cases when only cosine or sine part of the ringdown waves are considered. In Appendix B, we discuss the number of templates in the case when the mass of the black hole is known.

## II. QUASINORMAL RINGING MODES

A black hole is characterized by its mass  $M$  and spin angular momentum  $J$ . Here we use the dimensionless spin

parameter  $a = J/M^2$  that takes a value in the range  $[0, 1)$  with  $a = 0$  corresponding to a Schwarzschild black hole and  $a = 1$  to extreme Kerr black hole. Quasinormal modes of a black hole are complex frequency solutions of the Teukolsky wave equation that satisfy purely outgoing-wave boundary condition at infinity and ingoing-wave at horizon with vanishing incoming-wave amplitude. For fixed spheroidal harmonic indices  $(\ell, m)$ , there are infinite number of quasinormal modes. They are assigned with an index  $n$  with the order of the magnitude of the imaginary part, i.e., the  $n = 1$  mode has the smallest imaginary part (or the largest quality factor). We call it the least-damped (fundamental) mode. It is known that the imaginary part of the  $\ell = m = 2$  least-damped mode is the smallest of all the quasinormal modes, and results of black hole perturbation calculations as well as numerical relativity simulations strongly suggest that the ringdown waves are dominated by this  $\ell = m = 2$  least-damped mode unless the spin parameter  $a$  is extremely close to unity. Hence, we focus on this mode.

For the  $\ell = m = 2$  least-damped mode, analytical fitting formulas for the central frequency and quality factor for a black hole of mass  $M$  and dimensionless spin  $a$  were found by Echeverria as

$$f_c \approx 32 \text{ kHz} [1 - 0.63(1 - a)^{0.3}] \left( \frac{M}{M_\odot} \right)^{-1}, \quad (2.1)$$

$$Q \approx 2.0(1 - a)^{-0.45}. \quad (2.2)$$

The ringdown waveform is expressed as

$$h(f_c, Q, t_0, \phi_0; t) = \begin{cases} e^{-\pi f_c(t-t_0)/Q} \cos(2\pi f_c(t-t_0) - \phi_0) & \text{for } t \geq t_0, \\ 0 & \text{for } t < t_0, \end{cases} \quad (2.3)$$

where  $t_0$  and  $\phi_0$  are the initial time and phase of the ringdown wave, respectively.

## III. TEMPLATE SPACE

In this section, we develop an efficient technique of template spacing which can be used for matched filtering of the quasinormal ringing waveforms. Here, the detector noise is assumed to be white noise to make it possible to deal with the problem analytically. The case of the colored noise is discussed in the next section.

### A. Distance function

We have temporarily set the amplitude to unity for simplicity in Eq. (2.3). Note that the knowledge of the amplitude is not necessary for the template spacing in matched filtering. For  $t \geq t_0$ , the ringdown wave (2.3) is divided into two parts:

$$h(f_c, Q, t_0, \phi_0; t) = h_c(f_c, Q, t_0; t) \cos \phi_0 + h_s(f_c, Q, t_0; t) \sin \phi_0, \quad (3.1)$$

where

$$h_c(f_c, Q, t_0; t) = e^{-\pi f_c(t-t_0)/Q} \cos(2\pi f_c(t-t_0)), \quad (3.2)$$

$$h_s(f_c, Q, t_0; t) = e^{-\pi f_c(t-t_0)/Q} \sin(2\pi f_c(t-t_0)). \quad (3.3)$$

Performing the Fourier transformation  $\tilde{h}_{c/s}(f) = \int_{-\infty}^{\infty} dt e^{2\pi i f t} h_{c/s}(t)$ , we obtain the waveform in the frequency domain as

$$\tilde{h}_c(f_c, Q, t_0; f) = \frac{(f_c - 2ifQ)Q e^{2i\pi f t_0}}{\pi(2f_c Q - if_c - 2fQ)(2f_c Q + if_c + 2fQ)}, \quad (3.4)$$

$$\tilde{h}_s(f_c, Q, t_0; f) = \frac{2f_c Q^2 e^{2i\pi f t_0}}{\pi(2f_c Q - if_c - 2fQ)(2f_c Q + if_c + 2fQ)}. \quad (3.5)$$

The waveform in the time domain is real, so the following relation is satisfied:

$$\tilde{h}^*(f) = \tilde{h}(-f), \quad (3.6)$$

where the star (\*) denotes the complex conjugation.

Here, we introduce the inner product between two functions as

$$(a, b) = \int_{-f_{\max}}^{f_{\max}} df \tilde{a}(f) \tilde{b}^*(f), \quad (3.7)$$

where  $f_{\max}$  is the maximum frequency we take into account in the analysis. In the actual data analysis, it is equal to or less than the half of the sampling frequency of data.

In the matched filtering, we calculate the inner product between the template  $h$  and the signal  $x$  defined by  $(x, h)$ . We

first introduce the normalized template. We define the normalization constants as

$$\begin{aligned} N_c(f_c, Q, t_0) &= (\tilde{h}_c(f_c, Q, t_0), \tilde{h}_c(f_c, Q, t_0)) \\ &= \frac{1}{2} \frac{(2Q^2 + 1)Q}{\pi(4Q^2 + 1)f_c}, \end{aligned} \quad (3.8)$$

$$\begin{aligned} N_s(f_c, Q, t_0) &= (\tilde{h}_s(f_c, Q, t_0), \tilde{h}_s(f_c, Q, t_0)) \\ &= \frac{Q^3}{\pi(4Q^2 + 1)f_c}, \end{aligned} \quad (3.9)$$

when we set  $f_{\max} = \infty$ . The normalized templates  $\hat{h}_{c/s}(f_c, Q, t_0; f)$  are given by

$$\hat{h}_{c/s}(f_c, Q, t_0; f) = \frac{1}{\sqrt{N_{c/s}(f_c, Q, t_0)}} \tilde{h}_{c/s}(f_c, Q, t_0; f). \quad (3.10)$$

We then consider  $\hat{h} = \hat{h}_c \cos \phi_0 + \hat{h}_s \sin \phi_0$  as a template. We note that the  $h_c$  and  $h_s$  are not orthogonal. Their inner product is given by

$$\begin{aligned} (\hat{h}_c(f_c, Q, t_0), \hat{h}_s(f_c, Q, t_0)) &= \frac{1}{\sqrt{2(2Q^2 + 1)}} \\ &=: c(f_c, Q, t_0), \end{aligned} \quad (3.11)$$

when  $f_{\max} = \infty$ . In this case, the maximization of  $(x, \hat{h})$  over the phase  $\phi_0$  can be carried out analytically to yield [18]

$$\Lambda(x) \equiv \max_{\phi_0} (x, \hat{h}) = \frac{(x, \hat{h}_c(f_c, Q, t_0))^2 + (x, \hat{h}_s(f_c, Q, t_0))^2 - 2c(f_c, Q, t_0)(x, \hat{h}_c(f_c, Q, t_0))(x, \hat{h}_s(f_c, Q, t_0))}{1 - c(f_c, Q, t_0)^2}. \quad (3.12)$$

In the following, we consider the 3-dimensional template space  $\{f_c, Q, t_0\}$ .

Here we consider the match  $C(df_c, dQ, dt_0)$  between the template with  $(f_c, Q, t_0)$  and the normalized signal having slightly different sets of the parameters  $(f_c + df_c, Q + dQ, t_0 + dt_0)$ . Since we have already maximized over the phase  $\phi_0$  in  $\Lambda$ , without losing generality, we only need to consider  $\hat{h}_c$  for the signal. Then, the match is defined by

$$\begin{aligned} C(df_c, dQ, dt_0) &= \Lambda(\hat{h}_c(f_c + df_c, Q + dQ, t_0 + dt_0)) \\ &= 1 - \frac{2Q^4}{(2Q^2 + 1)f_c^2} df_c^2 - \frac{2Q^2(4Q^2 + 5)}{(4Q^2 + 1)^2(2Q^2 + 1)} dQ^2 - \frac{2Q^2}{f_c(4Q^2 + 1)(2Q^2 + 1)} df_c dQ \\ &\quad + \frac{4\pi f_c(1 + 4Q^2)f_{\max}}{Q(2Q^2 + 1)} dt_0^2 + \frac{\pi f_c}{2Q^2 + 1} dt_0 dQ, \end{aligned} \quad (3.13)$$

where we have used the approximation  $f_{\max} \gg f_c$ , and only the leading term in  $f_{\max}/f_c$  are shown. We will find that the dependence of  $f_{\max}$  will be cancelled out and does not appear in the final result. The inequality  $C(df_c, dQ, dt_0) \leq 1$  means that there will be a loss of signal-to-noise ratio unless the actual parameters of a gravitational wave signal fall exactly onto one of the templates.

The smaller the match  $C$  is, the larger the distance is between the two signals in the template space. Therefore, we define the metric in the template space by  $ds_{(3)}^2 = 1 - C$  [19], that is,

$$\begin{aligned} ds_{(3)}^2 &= g_{ij}^{(3)} dx^i dx^j \\ &= \frac{2Q^4}{(2Q^2+1)f_c^2} df_c^2 + \frac{2Q^2(4Q^2+5)}{(4Q^2+1)^2(2Q^2+1)} dQ^2 \\ &\quad - \frac{2Q^3}{f_c(4Q^2+1)(2Q^2+1)} df_c dQ \\ &\quad + \frac{4\pi f_c(1+4Q^2)f_{\max}}{Q(2Q^2+1)} dt_0^2 + \frac{\pi f_c}{2Q^2+1} dt_0 dQ. \end{aligned} \quad (3.14)$$

### B. Projection to 2-dimensional template space

Now to maximize the match with respect to  $dt_0$ , we consider a projection of the distance function into two dimensions spanned by  $f_c$  and  $Q$ . Namely, we project  $g_{ij}^{(3)}$  to a two dimensional subspace orthogonal to the  $t_0$  axis [19] as

$$g_{IJ}^{(2)} = g_{IJ}^{(3)} - \frac{g_{It_0}^{(3)} g_{Jt_0}^{(3)}}{g_{t_0 t_0}^{(3)}}, \quad (3.15)$$

where the indices  $I, J$  are  $\{f_c, Q\}$ . So, we find

$$\begin{aligned} ds_{(2)}^2 &= g_{IJ}^{(2)} dx^I dx^J = \frac{2Q^4}{(2Q^2+1)f_c^2} df_c^2 \\ &\quad + \frac{2Q^2(4Q^2+5)}{(4Q^2+1)^2(2Q^2+1)} dQ^2 \\ &\quad - \frac{2Q^3}{f_c(4Q^2+1)(2Q^2+1)} df_c dQ, \end{aligned} \quad (3.16)$$

where we have taken the limit  $f_{\max} \rightarrow \infty$ .

It is noted that the cross term  $df_c dQ$  arises here. Later, we discuss a coordinate transformation in the template space that removes the cross term, in order to make our analysis of the template spacing and the error estimation easier. We also note that the dependence of the metric on  $f_c$  can be eliminated by the simple coordinate transformation  $f_c \rightarrow \ln f_c$ .

It is also noted that the smaller the volume element of the metric is the fewer the number of required filters is to cover the template space.

The metric in the case of only  $h_c$  or  $h_s$  as templates is discussed in Appendix A.

### C. Diagonalization of the metric

Let us perform the coordinate transformation by which the two dimensional metric (3.16) is transformed to a diagonal, conformally flat metric.

We start from the coordinate transformation that removes the frequency dependence in the metric. We set

$$dF = \frac{df_c}{f_c}, \quad (3.17)$$

which gives

$$\begin{aligned} ds^2 &= g_{FF} dF^2 + g_{QQ} dQ^2 + 2g_{FQ} dF dQ \\ &= \frac{2Q^4}{(2Q^2+1)} dF^2 + \frac{2Q^2(4Q^2+5)}{(4Q^2+1)^2(2Q^2+1)} dQ^2 \\ &\quad - \frac{2Q^3}{(4Q^2+1)(2Q^2+1)} dF dQ. \end{aligned} \quad (3.18)$$

The transformation that removes the off-diagonal element is found by setting  $F = X - u(Q)$  and requiring

$$g_{FF} u'(Q) - g_{FQ} = 0. \quad (3.19)$$

We find

$$u = \frac{1}{2} \ln \left( 4 + \frac{1}{Q^2} \right), \quad (3.20)$$

which gives

$$\begin{aligned} ds^2 &= g_{FF} dX^2 + (g_{FF} u'^2 - 2g_{FQ} u' + g_{QQ}) dQ^2 \\ &= g_{FF} \left( dX^2 + \frac{g_{FF} g_{QQ} - g_{FQ}^2}{g_{FF}^2} dQ^2 \right). \end{aligned} \quad (3.21)$$

Then we can perform a further coordinate transformation to make the metric conformally flat. Namely, by the transformation  $Q \rightarrow Y$  defined by

$$Y = \int_Q^\infty dQ' \sqrt{\frac{\det g(Q')}{g_{FF}(Q')}} = \int_Q^\infty dx \sqrt{\frac{x+1}{x(4x+1)}} \quad (Q > 0), \quad (3.22)$$

we obtain

$$ds^2 = \Omega(Y) (dX^2 + dY^2), \quad (3.23)$$

where the conformal factor is given by

$$\Omega(Y) = g_{FF}(Q(Y)). \quad (3.24)$$

Here  $Q$  is now a function of  $Y$  determined by inverting Eq. (3.22).

Although the above coordinate transformation involves complicated functions that may not be expressed in terms of elementary functions, we find it is sufficient to use their large  $Q$  expansion forms for  $Q \geq 2$ . Up to  $O(1/Q^8)$  inclusive, we have

$$X = F + u = F + \ln 2 + \frac{1}{8} \frac{1}{Q^2} - \frac{1}{64} \frac{1}{Q^4} + \frac{1}{384} \frac{1}{Q^6} - \frac{1}{2048} \frac{1}{Q^8}, \quad (3.25)$$

$$Y = \frac{1}{2} \frac{1}{Q} + \frac{1}{24} \frac{1}{Q^3} - \frac{3}{160} \frac{1}{Q^5} + \frac{1}{128} \frac{1}{Q^7} - \frac{17}{4608} \frac{1}{Q^9}. \quad (3.26)$$

To the same accuracy, the inverse transformation becomes

$$F = X - \ln 2 - \frac{1}{2} Y^2 + \frac{7}{12} Y^4 - \frac{67}{45} Y^6 + \frac{1769}{360} Y^8, \quad (3.27)$$

$$Q = \frac{1}{2} \frac{1}{Y} + \frac{1}{6} Y - \frac{37}{90} Y^3 + \frac{166}{135} Y^5 - \frac{5917}{1350} Y^7. \quad (3.28)$$

The conformal factor  $\Omega(Y)$  is given by

$$\Omega(Y) = \frac{1}{4} \frac{1}{Y^2} - \frac{1}{3} + \frac{37}{60} Y^2 - \frac{85}{54} Y^4 + \frac{13\,069}{2700} Y^6. \quad (3.29)$$

When  $Q=2$ , the errors induced by the above expansion are found to be  $\sim 0.1\%$ . This is accurate enough for our purpose as long as we allow the SNR loss,  $ds_{\max}^2$ , of a few percent.

#### D. Tiling method: basis

In the previous subsection, we have derived the simple, conformally flat metric (3.23) for the template space. Here, using this metric, we formulate a tiling algorithm which is not only efficient but also quite simple.

To develop such a method, we note the following. Because of the conformal flatness, the contour of the fixed maximum distance  $ds^2 = ds_{\max}^2$  centered at a point on the  $(X, Y)$  plane is a circle for sufficiently small  $ds_{\max}^2$ . Furthermore, along a line of  $Y = \text{const}$ ,  $\Omega(Y)$  is constant. Thus, choosing first an appropriate  $Y = \text{const}$  line, say  $Y = q_1$ , we may place circles of the same radius with their centers located along the line  $Y = q_1$  to cover a region surrounding that line. Then, if we find an algorithm to place circles along the  $Y = q_1$  line and another algorithm to choose the next  $Y = \text{const}$  line, say  $Y = q_2$ , to be covered in an appropriate way, we can repeat this tiling procedure to cover the whole template space.

Let us assume that the template space to be tiled is a rectangle given by  $F_{\min} \leq F \leq F_{\max}$  and  $Q_{\min} \leq Q \leq Q_{\max}$ . In the  $(X, Y)$  coordinates, this rectangle is mapped to the region bounded by the two  $Y = \text{const}$  lines corresponding to  $Q = Q_{\min}$  and  $Q = Q_{\max}$ , which we denote by  $Y = Y_0$  and  $Y_M$ , respectively, and the two lines  $X = v_{\min}(Y)$  and  $X = v_{\max}(Y)$  corresponding to  $F = F_{\min}$  and  $F = F_{\max}$ , respectively. Note

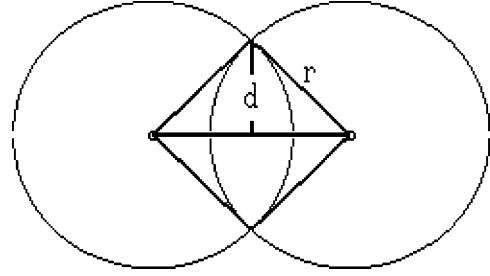


FIG. 1. Definition of  $d$  and  $r$ .

that  $Y_0 > Y_M$  since large  $Y$  corresponds to small  $Q$ .

First, we construct a method to determine the spacing of the circles along each  $Y = \text{const}$  line. Let us consider the line  $Y = q$  and place two circles with radius  $r$  centered at  $(p, q)$  and  $(p + \Delta p, q)$ ,

$$(X - p)^2 + (Y - q)^2 = r^2, \quad (X - p - \Delta p)^2 + (Y - q)^2 = r^2. \quad (3.30)$$

We assume  $\Delta p < 2r$  so that the two circles intersect at the two points,  $(p + \Delta p/2, q \pm d(r; p))$ , where  $d(r; p)$  is the distance to each intersecting point from the line  $Y = q$  (see Fig. 1), given by

$$d(r; \Delta p) = \sqrt{r^2 - \frac{\Delta p^2}{4}}. \quad (3.31)$$

Our purpose is to tile the template space by the smallest possible number of filters. In order to do so, we choose the parameter  $p$  in such a way that the area defined by  $S = \Delta p d(r; \Delta p)$  is maximized, i.e.,

$$\Delta p = \sqrt{2}r, \quad (3.32)$$

$$d = \frac{r}{\sqrt{2}}. \quad (3.33)$$

The radius  $r$  is determined by the value of  $ds_{\max}^2$  and  $q$  as

$$r^2 = \frac{ds_{\max}^2}{\Omega(q)}. \quad (3.34)$$

In this way, we tile the region that covers the line  $Y = q$ .

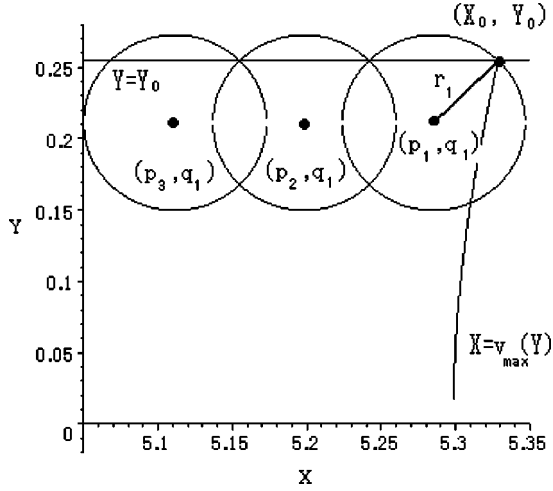
To choose the first line to be covered, we start from the point on the  $(X, Y)$  plane corresponding to  $(F, Q) = (F_{\max}, Q_{\min})$ , that is,  $(X, Y) = (X_0, Y_0)$  where  $X_0 = v_{\max}(Y_0)$ . Then we choose the first line  $Y = q_1$  and the radius  $r_1$  so that the point  $(X_0, Y_0)$  is just on the edge of the first circle and an intersecting point of the first and second circles lies on the line  $Y = Y_0$  as Fig. 2. This is achieved if the center of the first circle is at

$$(p_1, q_1) = (X_0 - r_1/\sqrt{2}, Y_0 - r_1/\sqrt{2}), \quad (3.35)$$

with the radius determined by solving Eq. (3.34), which reads in the present case,

$$ds_{\max}^2 = r_1^2 \Omega(Y_0 - r_1/\sqrt{2}). \quad (3.36)$$

Then the center of the  $n$ th circle is at


 FIG. 2. Choosing the first line on the  $(X, Y)$  plane.

$$(p_n, q_1) = (X_0 - (2n - 1)r_1/\sqrt{2}, Y_0 - r_1/\sqrt{2}), \quad (3.37)$$

and the number of circles needed to cover the line  $Y = q_1$  is given by

$$N_1 = \left\lceil \frac{L_1}{\sqrt{2}r_1} \right\rceil, \quad (3.38)$$

where  $\lceil x \rceil$  denotes the maximum integer smaller than  $x + 1$  and  $L_1$  is the coordinate length of  $X$  to be covered, i.e.,

$$\begin{aligned} L_1 &= v_{\max}(Y_0) - v_{\min}(Y_0) \\ &= F_{\max} - F_{\min} \\ &=: L. \end{aligned} \quad (3.39)$$

Once the covering of the first line is done, the second  $Y = \text{const}$  line is chosen as follows. Let  $Y_1 = Y_0 - \sqrt{2}r_1$  and let  $(X_1, Y_1)$  be the intersecting point of the lines  $Y = Y_1$  and  $X = v_{\max}(Y)$ , i.e.,  $(X_1, Y_1) = (v_{\max}(Y_1), Y_1)$ . We choose this point as the starting point for the covering of the second line as Fig. 3. That is, the center of the first circle  $(p_2, q_2)$  on the

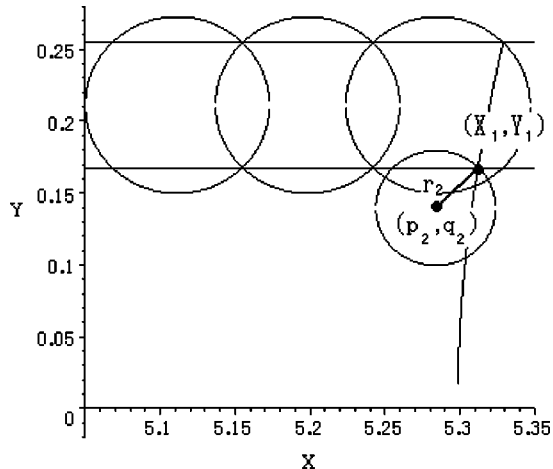


FIG. 3. Covering of the second line.

second line  $Y = q_2$  is

$$(p_2, q_2) = (X_1 - r_2/\sqrt{2}, Y_1 - r_2/\sqrt{2}), \quad (3.40)$$

with the radius  $r_2$  determined again by Eq. (3.34). Then the second line is covered by the same procedure we took for the first line. We repeat this procedure until we tile the whole template space we need to cover.

With this tiling procedure, the total number of templates is given as follows. Generalizing Eq. (3.38), the number of templates for the  $i$ th  $Y = \text{const}$  line ( $Y = q_i$ ) is

$$N_i = \left\lceil \frac{L}{\sqrt{2}r_i} \right\rceil, \quad (3.41)$$

where  $r_i$  is determined by

$$ds_{\max}^2 = r_i^2 \Omega(Y_{i-1} - r_i/\sqrt{2}). \quad (3.42)$$

The number of  $Y = \text{const}$  lines necessary to cover the template space is determined by the minimum integer  $\nu$  that satisfies the inequality,

$$\sum_{i=1}^{\nu} \sqrt{2}r_i \geq Y_0 - Y_M. \quad (3.43)$$

And the total number of templates is

$$N = \sum_{i=1}^{\nu} N_i. \quad (3.44)$$

### E. Tiling method: application

Let us apply the method developed in the previous subsection to the case of the parameter space  $(f_c, Q)$  which has the range

$$\begin{aligned} 10^2 \text{ Hz} &\leq f_c \leq 10^4 \text{ Hz}, \\ 2 &\leq Q \leq 20. \end{aligned} \quad (3.45)$$

We set  $ds_{\max}^2 = 0.02$ . This choice is made in order to make the SNR loss to be  $\sim 3\%$  in the presence of colored noise as discussed in the next section. Using Eq. (3.17), we set  $F = \ln(f_c/100 \text{ Hz})$ . The above range corresponds to

$$\begin{aligned} 6.93 \times 10^{-1} &\leq X \leq 5.33, \\ 2.50 \times 10^{-2} &\leq Y \leq 2.55 \times 10^{-1}, \end{aligned} \quad (3.46)$$

in the  $(X, Y)$  space. (See Table I.)

Following the procedure described in the previous subsection, we choose the starting point  $(X_0, Y_0)$  which corresponds to  $(f_c, Q) = (10^4 \text{ Hz}, 2.0)$ . The radius  $r_1$  is determined by Eq. (3.36), or

$$0.02 = r_1^2 \Omega(Y_0 - r_1/\sqrt{2}). \quad (3.47)$$

Then all the parameters for our tiling method are determined. In Table II, we summarize the tiling parameters.

TABLE I. The relation between the two coordinates.

$(f_c, Q)$	$(X, Y)$
$10^2$ Hz, 2.0	$7.234\ 594\ 008 \times 10^{-1}, 2.546\ 762\ 255 \times 10^{-1}$
$10^2$ Hz, 20.0	$6.934\ 595\ 830 \times 10^{-1}, 2.500\ 520\ 248 \times 10^{-2}$
$10^3$ Hz, 2.0	$3.026\ 044\ 494, 2.546\ 762\ 255 \times 10^{-1}$
$10^3$ Hz, 20.0	$2.996\ 044\ 676, 2.500\ 520\ 248 \times 10^{-2}$
$10^4$ Hz, 2.0	$5.328\ 629\ 588, 2.546\ 762\ 255 \times 10^{-1}$
$10^4$ Hz, 20.0	$5.298\ 629\ 769, 2.500\ 520\ 248 \times 10^{-2}$

It is noted that the number  $\nu$  of the  $Y = \text{const}$  lines is very small,

$$\nu = 6. \quad (3.48)$$

The total number of templates is calculated to be  $\mathcal{N} = 1148$  ( $\mathcal{N} = 1780$  for  $Q_{\text{max}} = 34.3$ ). In Fig. 4, we show the tiling of the template space in the  $(X, Y)$  coordinates (see also Fig. 5). The tiling of the template space in the original coordinates  $(f_c, Q)$  is shown in Fig. 6. (See also Fig. 7.)

In order to see how effective this tiling method is, we calculate the ratio between the sum of the areas of all the circles  $\mathcal{S}_{\text{cir}}$  and the area to be covered  $\mathcal{S}_{\text{par}}$ . We find

$$\begin{aligned} \eta &= \frac{\mathcal{S}_{\text{cir}}}{\mathcal{S}_{\text{par}}} \\ &= 1.57. \end{aligned} \quad (3.49)$$

Here we have adopted  $Q_{\text{max}} = 22.9$  which is slightly larger than the preassigned value of  $Q_{\text{max}} = 20$ . The former value corresponds to the value  $Y = q_6 - r_6 / \sqrt{2}$ , i.e., the value of the  $Y = \text{const}$  line marginally covered by the circles centered along the line  $Y = q_6$ . This ratio corresponds to  $\eta_{\text{tot}}$  in the paper by Arnaud *et al.* [17], in which they obtained  $\eta_{\text{tot}} = 2.12$  for their tiling method. Thus our tiling method is far more efficient (and simpler) than that of Arnaud *et al.*

#### IV. VALIDITY OF TILING METHOD IN THE CASE OF COLORED NOISE SPECTRUM

The tiling method discussed in the previous section is based on an assumption that the noise is white. We expect

TABLE II. The parameters for the tiling of the template space are summarized.  $(X_i, Y_i)$  denotes the starting point of the  $i$ th template spacing along the line  $y = q_i$ .  $(p_i, q_i)$  denotes the center of the first circle along the  $i$ th line  $y = q_i$ ,  $r_i$  is the radius of the circle, and  $N_i$  is the number of circles necessary to cover the  $i$ th line.

$i$	$(p_i, q_i)$	$(X_i, Y_i)$	$r_i$	$N_i$
0		$5.328\ 629\ 588, 2.546\ 762\ 255 \times 10^{-1}$		
1	$5.285\ 172\ 504, 2.112\ 191\ 414 \times 10^{-1}$	$5.311\ 957\ 476, 1.677\ 620\ 573 \times 10^{-1}$	$6.145\ 759\ 769 \times 10^{-2}$	53
2	$5.283\ 700\ 230, 1.395\ 048\ 115 \times 10^{-1}$	$5.304\ 418\ 737, 1.112\ 475\ 658 \times 10^{-1}$	$3.996\ 178\ 019 \times 10^{-2}$	82
3	$5.285\ 789\ 828, 9.261\ 865\ 694 \times 10^{-2}$	$5.301\ 037\ 366, 7.398\ 974\ 808 \times 10^{-2}$	$2.634\ 525\ 556 \times 10^{-2}$	124
4	$5.288\ 679\ 812, 6.163\ 219\ 420 \times 10^{-2}$	$5.299\ 527\ 944, 4.927\ 464\ 032 \times 10^{-2}$	$1.747\ 622\ 029 \times 10^{-2}$	187
5	$5.291\ 307\ 826, 4.105\ 452\ 276 \times 10^{-2}$	$5.298\ 855\ 740, 3.283\ 440\ 519 \times 10^{-2}$	$1.162\ 500\ 174 \times 10^{-2}$	281
6	$5.293\ 381\ 065, 2.735\ 973\ 019 \times 10^{-2}$		$7.742\ 359\ 638 \times 10^{-3}$	421

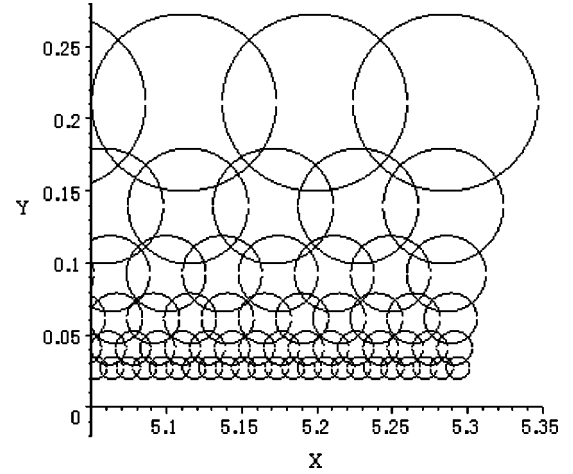


FIG. 4. A part of the tiling of the template space in the  $(X, Y)$  coordinates. Templates are taken at the centers of the circles.

this assumption is very good because the ringing wave is rather narrow banded except the case  $Q \sim 2$ . In order to confirm this, we examine the effectiveness of the tiling method in the case of colored noise.

As a model of detector's noise, we use a fitting curve of the one sided noise power spectrum of TAMA300, which is given by

$$\begin{aligned} S_n(|f|) &= \left(\frac{85}{f}\right)^{63} + \frac{1}{2} \left(\frac{220}{f}\right)^{10} + \frac{1}{9} \left(\frac{710}{f}\right)^3 \\ &\quad + \frac{3}{20} + \frac{1}{20} \left(\frac{f}{2000}\right)^2 + \frac{1}{5} \left(\frac{f}{5500}\right)^6. \end{aligned} \quad (4.1)$$

This formula of the noise spectrum is obtained by fitting Fig. 3.4.1 in TAMA REPORT 2002 [20] which is based on the spectrum during Data Taking 7 in 2002, and is valid between 60 Hz and 40000 Hz. Here we have ignored the overall amplitude of  $S_n$ , because it does not affect the results.

We prepare the template bank using the analytical method in the white noise case. The minimal match is assumed to be 0.98. We also generate signals which are normalized to unity. We then calculate the maximum of the match between the signal and templates. When the signal is completely the same, the match becomes unity. However, we have the match less than unity due to mismatch between signal and tem-

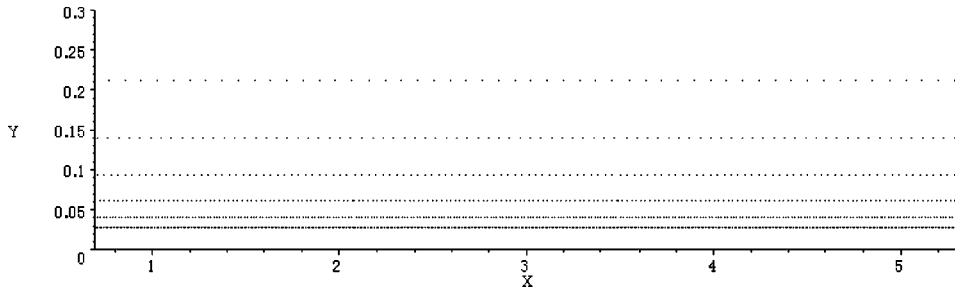


FIG. 5. The template points on the  $(X, Y)$  plane. It is noted that we may put the templates with the same interval along the  $X$  direction.

plates. If the match is always greater than 0.98, we have a justification to use the tiling method even in the case of the colored noise spectrum.

We used 2500 signals. The range of the central frequency  $f_c$  and the  $Q$  value of the signals are  $100 \text{ Hz} \leq f_c \leq 10^4 \text{ Hz}$  and  $2 \leq Q \leq 20$  respectively. The value of  $f_c$  and  $Q$  are randomly given in this region.

In Fig. 8, we show the number of signals in terms of the value of the match.

From Fig. 8, we find that we can detect the most of the signals without losing 2% of the signal-to-noise ratio by the tiling method assuming white noise. Thus, the tiling method, constructed analytically assuming white noise, is valid even in the case of the TAMA noise spectrum.

## V. DISCUSSION

In this paper, we proposed a tiling method of the template space in the matched filtering search for the gravitational waves of black hole ringing.

First, we discussed a tiling method assuming the detector noise is white. We found that the  $1/Q$  expansion was useful

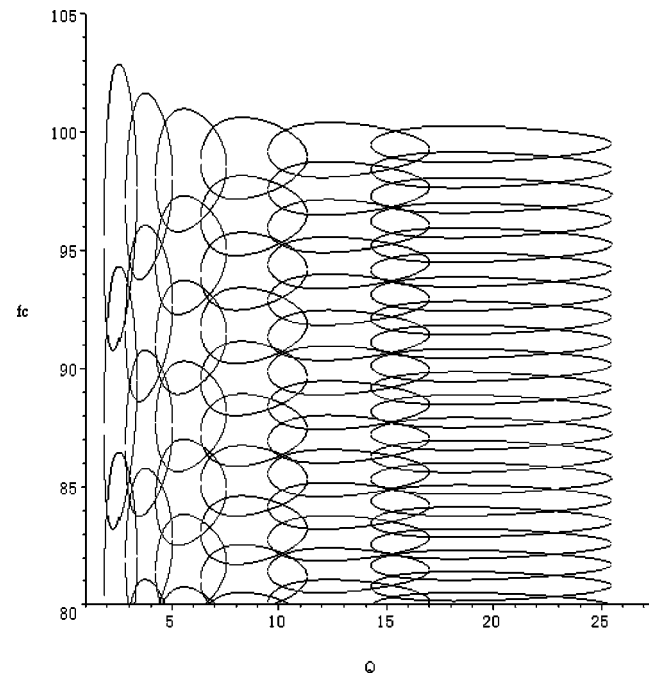


FIG. 6. A part of the tiling of the template space in the original coordinates  $(f_c, Q)$  with  $f_c$  measured in units of 100 Hz. Note that the contour of  $ds_{\text{max}}^2 = 0.02$  for each template is warped.

in performing the coordinate transformation of the metric of the template space because of  $Q \geq 2$ . We also find an efficient tiling method of the template space which can be formulated analytically. When the range of  $f_c$  and  $Q$  is  $10^2 \leq f_c \leq 10^4 \text{ Hz}$  and  $2 \leq Q \leq 20$ , and the minimal match is 0.97, the ratio  $\eta$ , between the sum of the areas of the equal match circles around the templates,  $\mathcal{S}_{\text{cir}}$ , and the area to be covered,  $\mathcal{S}_{\text{par}}$ , is 1.57 which is much smaller than the value obtained before.

Next, we have discussed the validity of this tiling method in the case of colored noise spectrum. As a model of realistic noise power spectrum, we used a fitting curve of the noise power spectrum of TAMA300 during 2002. We prepare a template bank assuming the minimum match 98%. We then examined the loss of signal-to-noise ratio of the signals detected in the template bank. We found that, in most case, we do not lose the signal-to-noise ratio no more than 2% which is expected from the preassigned minimum match. This shows that the tiling method can be used even in the case of colored noise spectrum.

The tiling method should be tested using the real data of laser interferometers. A study in this direction using the data of TAMA300 is now progressing [21].

In the analysis using real interferometers' data, we have to treat the nonstationary, non-Gaussian noise. It is found [22] that we observe even more fake events than in the case of inspiraling wave, since the ringing wave is usually much shorter than the inspiral waves and can easily be affected by short bursts. In this situation, we would need to introduce some methods to remove such fake events without losing real ringing gravitational wave signals. Coincidence analysis between several detectors would also be needed to reduce the fake event rate. Further, since the ringing waves may be excited by the detector itself, we may need to perform coincidence analysis to reject such spurious events anyway. We will also work on this problem in the future.

## ACKNOWLEDGMENT

We would like to thank N. Kanda and Y. Tsunesada for useful discussions and comments. H.N. is supported by the Japan Society for the Promotion of Science for Young Scientists, No. 5919. This work is supported in part by Monbukagakaku-sho Grant-in-Aid for Scientific Research No. 14047214 and 12640269.

## APPENDIX A: THE METRIC IN SOME SPECIAL CASES

In this appendix, we summarize the distance function in the case when we consider only the cosine or sine part of the

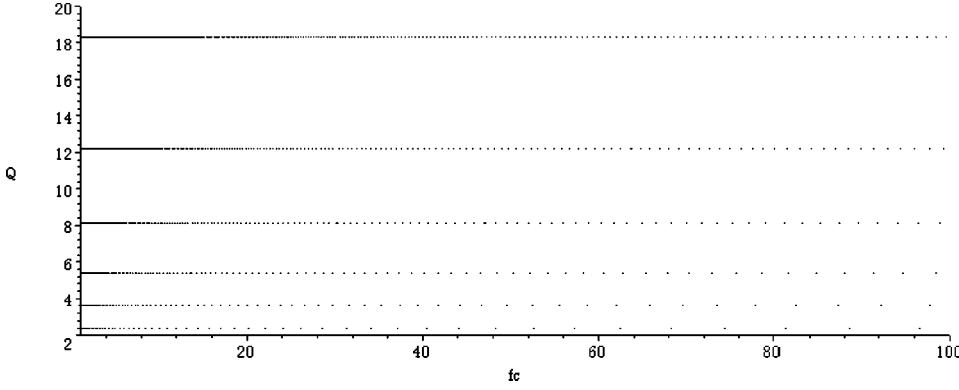


FIG. 7. The template points on the original coordinates  $(f_c, Q)$ . The smaller the value of  $f_c$  is, the larger the number of templates is needed.

wave, ignoring the contribution of the phase and the initial time. We also consider the case when the detector noise is white. Although the applicability of such special cases will be limited, we describe them here because there are still some cases when these formulas become useful.

### 1. Cosine wave case

We consider the cosine waveform ignoring the initial time and phase of a ringdown wave,

$$h(f_c, Q; t) = \begin{cases} e^{-\pi f_c t / Q} \cos(2\pi f_c t) & \text{for } t \geq 0, \\ 0 & \text{for } t < 0. \end{cases} \quad (\text{A1})$$

Performing the Fourier transformation  $\tilde{h}(f) = \int_{-\infty}^{\infty} dt e^{2\pi i f t} h(t)$ , we obtain the waveform in the frequency domain as

$$\tilde{h}(f_c, Q; f) = \frac{(f_c - 2ifQ)Q}{\pi(2f_cQ - if_c - 2fQ)(2f_cQ + if_c + 2fQ)}. \quad (\text{A2})$$

In the following, we consider normalized waveforms. The normalization constant is derived as

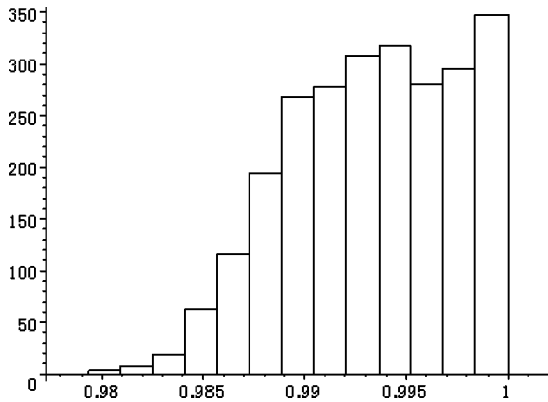


FIG. 8. The number of signals in terms of the value of the match between the signal and templates. The bank of templates are determined assuming the minimum match 0.98 using the method in Sec. III. The mean value of the match is 0.993.

$$N(f_c, Q) = \int_{-\infty}^{\infty} |\tilde{h}(f_c, Q; f)|^2 df = \frac{1}{2} \frac{(2Q^2 + 1)Q}{\pi(4Q^2 + 1)f_c}. \quad (\text{A3})$$

With the above normalization constant, the normalized wave  $\hat{h}(f_c, Q; f)$  is given by

$$\hat{h}(f_c, Q; f) = \frac{1}{\sqrt{N(f_c, Q)}} \tilde{h}(f_c, Q; f). \quad (\text{A4})$$

Now, we consider the correlation between the two normalized waves having slightly different sets of the parameters  $(f_c, Q)$  and  $(f_c + df_c, Q + dQ)$ ,

$$\begin{aligned} C(df_c, dQ) &= \int_{-\infty}^{\infty} df \hat{h}(f_c, Q; f) \hat{h}^*(f_c + df_c, Q + dQ; f) \\ &= 1 - \frac{1}{8} \frac{16Q^4 + 6Q^2 + 1}{(2Q^2 + 1)f_c^2} df_c^2 \\ &\quad - \frac{1}{8} \frac{64Q^8 + 128Q^6 + 28Q^4 + 1}{Q^2(4Q^2 + 1)^2(2Q^2 + 1)^2} dQ^2 \\ &\quad + \frac{1}{4} \frac{(8Q^4 + 2Q^2 + 1)}{f_c Q(4Q^2 + 1)(2Q^2 + 1)} df_c dQ. \end{aligned} \quad (\text{A5})$$

The inequality  $C(df_c, dQ) \leq 1$  means that there will be a loss of the signal to noise ratio unless the actual parameters of a gravitational wave signal fall exactly onto one of the templates.

The smaller the correlation  $C$  is, the larger the distance is between the two signals in the template space. Therefore, we define the metric in the template space by  $ds^2 = 1 - C$ , that is,

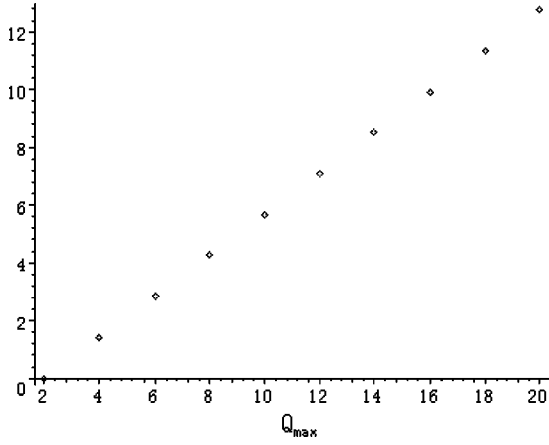


FIG. 9. The  $Q_{\max}$  dependence of the number of required filters  $[2ds_{\max}^2 N_f / \log(f_{\max}/f_{\min})]$ . Here we chose  $Q_{\min}=2$ .

$$\begin{aligned}
 ds^2 &= \frac{1}{8} \frac{16Q^4 + 6Q^2 + 1}{(2Q^2 + 1)f_c^2} df_c^2 \\
 &+ \frac{1}{8} \frac{64Q^8 + 128Q^6 + 28Q^4 + 1}{Q^2(4Q^2 + 1)^2(2Q^2 + 1)^2} dQ^2 \\
 &- \frac{1}{4} \frac{8Q^4 + 2Q^2 + 1}{f_c Q(4Q^2 + 1)(2Q^2 + 1)} df_c dQ, \quad (\text{A6})
 \end{aligned}$$

$$\begin{aligned}
 &\simeq \frac{Q^2}{f_c^2} df_c^2 + \frac{1}{8Q^2} dQ^2 - \frac{1}{4f_c Q} df_c dQ \\
 &\text{for large } Q. \quad (\text{A7})
 \end{aligned}$$

Note that the dependence of the metric on  $f_c$  can be eliminated by the simple coordinate transformation  $f_c \rightarrow \ln f_c$ . The metric in the case of the sine-wave templates instead of the cosine-wave templates (A1) is calculated in the next subsection. For large  $Q$ , the two metrics coincide with each other, implying that the phase effect is weak in the large  $Q$  limit.

The number of filters,  $N_f$ , which are required to achieve the detection efficiency determined by the maximum allowable distance  $ds_{\max}^2$  (i.e., the maximum allowable loss of SNR) in the region  $f_{\min} \leq f \leq f_{\max}$  and  $Q_{\min} \leq Q \leq Q_{\max}$  is estimated by integrating the volume element  $\sqrt{\det g}$  over that region of the template space. We find

$$\begin{aligned}
 N_f &= \frac{1}{2} (ds_{\max}^2)^{-1} \ln(f_{\max}/f_{\min}) \\
 &\times \int_{Q_{\min}}^{Q_{\max}} dQ \frac{Q(16Q^6 + 32Q^4 + 10Q^2 + 1)^{1/2}}{(2Q^2 + 1)^{3/2}(4Q^2 + 1)^{1/2}}. \quad (\text{A8})
 \end{aligned}$$

The  $Q_{\max}$  dependence of  $N_f$  is shown in Fig. 9. For large  $Q_{\max}$ , it can be derived analytically as [16]

$$N_f|_{\text{large-}Q} = \frac{\sqrt{2}}{4} (ds_{\max}^2)^{-1} \ln(f_{\max}/f_{\min}) Q_{\max}. \quad (\text{A9})$$

TABLE III. The estimation of the number of filters with the maximum SNR loss of 3%.

$f_{\max}(\text{Hz})$	$Q_{\max}=10$	$Q_{\max}=10^2$	$Q_{\max}=10^3$
$10^3$	218	2661	27 084
$10^4$	436	5321	54 167

From Fig. 9, we see that the large  $Q_{\max}$  approximation is good even for smaller  $Q_{\max}$  as far as the number of required filters is concerned. In Table III, we show the number of filters in the case  $Q_{\min}=2$ ,  $f_{\min}=100$  Hz, and  $ds_{\max}^2=0.03$  for several values of  $f_{\max}$  and  $Q_{\max}$ . We also note that the number of required filters depends on the choice of a tiling method in practice.

Next, let us perform the coordinate transformation by which the cosine-wave template metric (A6) is transformed to a diagonal, conformally flat metric.

We start from the coordinate transformation that removes the frequency dependence in the metric,

$$dF = d \ln f_c, \quad (\text{A10})$$

which gives

$$\begin{aligned}
 ds^2 &= g_{FF} dF^2 + g_{QQ} dQ^2 + 2g_{FQ} dF dQ \\
 &= \frac{1}{8} \frac{16Q^4 + 6Q^2 + 1}{(2Q^2 + 1)} dF^2 \\
 &+ \frac{1}{8} \frac{64Q^8 + 128Q^6 + 28Q^4 + 1}{Q^2(4Q^2 + 1)^2(2Q^2 + 1)^2} dQ^2 \\
 &- \frac{1}{4} \frac{8Q^4 + 2Q^2 + 1}{Q(4Q^2 + 1)(2Q^2 + 1)} dF dQ. \quad (\text{A11})
 \end{aligned}$$

The transformation that removes the off-diagonal element is found by setting  $F = X - u(Q)$  and requiring

$$g_{FF} u'(Q) - g_{FQ} = 0. \quad (\text{A12})$$

We find

$$\begin{aligned}
 u &= 3 \sqrt{\frac{7}{14}} \left[ \arctan\left(\frac{3 + 16Q^2}{\sqrt{7}}\right) - \frac{\pi}{2} \right] \\
 &- \frac{1}{4} \ln \frac{16Q^4(16Q^4 + 6Q^2 + 1)}{(4Q^2 + 1)^4}, \quad (\text{A13})
 \end{aligned}$$

which gives

$$\begin{aligned}
 ds^2 &= g_{FF} dX^2 + (g_{FF} u'^2 - 2g_{FQ} u' + g_{QQ}) dQ^2 \\
 &= g_{FF} \left( dX^2 + \frac{g_{FF} g_{QQ} - g_{FQ}^2}{g_{FF}^2} \right) dQ^2. \quad (\text{A14})
 \end{aligned}$$

Then we can perform a further coordinate transformation to make the metric conformally flat. Namely, by the transformation  $Q \rightarrow Y$  defined by

$$\begin{aligned}
Y &= \int_Q^\infty dQ' \sqrt{\frac{\det g(Q')}{g_{FF}(Q')}} \\
&= \int_Q^\infty dx 2 \sqrt{\frac{64x^4 + 144x^3 + 72x^2 + 14x + 1}{(64x^3 + 40x^2 + 10x + 1)\sqrt{1+2x}}} \quad (Q > 0),
\end{aligned} \tag{A15}$$

we obtain

$$ds^2 = \Omega(Y)(dX^2 + dY^2), \tag{A16}$$

where the conformal factor is given by

$$\Omega(Y) = g_{FF}(Q(Y)). \tag{A17}$$

Here  $Q$  is now a function of  $Y$  determined by inverting Eq. (A15).

Although the above coordinate transformation involves complicated functions that may not be expressed in terms of elementary functions, we find it is sufficient to use their large  $Q$  expansion forms for  $Q \geq 2$ . Up to  $O(1/Q^8)$  inclusive, we have

$$\begin{aligned}
X = F + u = F + \frac{1}{16} \frac{1}{Q^2} - \frac{3}{256} \frac{1}{Q^4} + \frac{13}{3072} \frac{1}{Q^6} \\
- \frac{43}{32768} \frac{1}{Q^8} + \frac{109}{327680} \frac{1}{Q^{10}},
\end{aligned} \tag{A18}$$

$$Y = \sqrt{\frac{2}{4}} \left( \frac{1}{Q} + \frac{1}{12} \frac{1}{Q^3} - \frac{73}{640} \frac{1}{Q^5} + \frac{21}{256} \frac{1}{Q^7} - \frac{6127}{98304} \frac{1}{Q^9} \right). \tag{A19}$$

To the same accuracy, the inverse transformation becomes

$$F = X - \frac{1}{2} Y^2 + \frac{17}{12} Y^4 - \frac{586}{45} Y^6 + \frac{47587}{360} Y^8 - \frac{3153013}{2025} Y^{10}, \tag{A20}$$

$$Q = \sqrt{\frac{2}{4}} \left( -\frac{4401959}{5400} Y^7 + \frac{9892}{135} Y^5 - \frac{737}{90} Y^3 + \frac{2}{3} Y + \frac{1}{Y} \right). \tag{A21}$$

The conformal factor  $\Omega(Y)$  is given by

$$\Omega(Y) = -\frac{749639}{5400} Y^6 + \frac{1255}{108} Y^4 - \frac{119}{120} Y^2 + \frac{1}{24} + \frac{1}{8} \frac{1}{Y^2}. \tag{A22}$$

The structure of this metric is the same as the one in the general case discussed in Sec. III. The effective tiling method describe in Sec. III can thus be used to set the template space using this metric.

## 2. Sine wave

Next, we consider the damped sine wave  $e^{-\pi f_c t/Q} \sin(2\pi f_c t)$ . The calculation is done as same as the cosine wave case. First, we obtain

$$\begin{aligned}
ds^2 &= \frac{1}{8} (8Q^2 + 3) dF^2 + \frac{1}{8} \frac{16Q^4 + 3}{Q^2(4Q^2 + 1)^2} dQ^2 \\
&\quad - \frac{1}{4} \frac{4Q^4 + 3}{Q(4Q^2 + 1)} dF dQ.
\end{aligned} \tag{A23}$$

For the above metric, the  $1/Q$  expansion is performed and we obtain

$$ds^2 = g_{FF} dF^2 + g_{QQ} dQ^2 + 2g_{FQ} dF dQ, \tag{A24}$$

$$g_{FF} = Q^2 + \frac{3}{8},$$

$$g_{QQ} = \frac{1}{8} \frac{1}{Q^2} - \frac{1}{16} \frac{1}{Q^4} + \frac{3}{64} \frac{1}{Q^6} - \frac{5}{256} \frac{1}{Q^8} + \frac{7}{1024} \frac{1}{Q^{10}},$$

$$g_{FQ} = -\frac{1}{8} \frac{1}{Q} - \frac{1}{16} \frac{1}{Q^3} + \frac{1}{64} \frac{1}{Q^5} - \frac{1}{256} \frac{1}{Q^7} + \frac{1}{1024} \frac{1}{Q^9}.$$

The expansion is considered up to  $O(1/Q^8)$  beyond the leading term.

Next, we consider the following coordinate transformation:

$$\begin{aligned}
X = F + \frac{1}{16} \frac{1}{Q^2} + \frac{1}{256} \frac{1}{Q^4} - \frac{11}{3072} \frac{1}{Q^6} \\
+ \frac{49}{32768} \frac{1}{Q^8} - \frac{179}{327680} \frac{1}{Q^{10}},
\end{aligned} \tag{A25}$$

$$Y = \sqrt{\frac{2}{4}} \left( \frac{1}{Q} - \frac{1}{6} \frac{1}{Q^3} + \frac{27}{640} \frac{1}{Q^5} - \frac{43}{3584} \frac{1}{Q^7} + \frac{1067}{294912} \frac{1}{Q^9} \right). \tag{A26}$$

The inverse transformation of this is given by

$$F = X - \frac{1}{2} Y^2 - \frac{19}{12} Y^4 - \frac{136}{45} Y^6 - \frac{15263}{2520} Y^8 - \frac{181651}{14175} Y^{10}, \tag{A27}$$

$$Q = \sqrt{\frac{2}{4}} \left( -\frac{71033}{37800} Y^7 - \frac{1073}{945} Y^5 - \frac{77}{90} Y^3 - \frac{4}{3} Y + \frac{1}{Y} \right). \tag{A28}$$

Finally, we obtain the conformally flat metric as

$$ds^2 = \Omega(Y)(dX^2 + dY^2), \quad (\text{A29})$$

$$\Omega(Y) = \frac{1}{5400}Y^6 + \frac{1}{756}Y^4 + \frac{1}{120}Y^2 + \frac{1}{24} + \frac{1}{8} \frac{1}{Y^2}. \quad (\text{A30})$$

The structure of this metric is the same as the one in the general case of Sec. III and the case of cosine wave. Especially, the leading term with respect to  $1/Q$  are the same as in the case of cosine wave. Therefore, the effective tiling method described in Sec. III is also applicable to this case.

#### APPENDIX B: THE NUMBER OF TEMPLATES WHEN THE MASS IS KNOWN

In this appendix, we consider the case when a compact star with mass  $1 \sim 10^2 M_\odot$  is inspiraling into a super massive black hole with mass  $10^6 \sim 10^8 M_\odot$ , and after the final plunge, the ringing wave is excited. In such cases, it is expected that masses of the super massive black hole and the compact star is determined accurately during the inspiral phase. We do not know exactly the mass of the final black hole after the plunge of the compact star because we do not know how much energy are radiated as the gravitational waves and how much mass loss will be occurred in the case of neutron star. In this case, however, we can assume the mass of the final black hole within the accuracy  $10^{-8} \sim 10^{-4}$  since the mass ratio is very large. In this case, we can

perform an analysis to search for the ringdown wave using these mass parameters. Here we investigate how much templates we need in this situation.

When we know the mass  $M$  of a black hole, we only need to investigate the spin of the black hole. From Eqs. (2.1) and (2.2), the relation between  $f_c$  and  $Q$  becomes

$$f_c \approx 320 \left[ 1 - 0.63 \left( \frac{Q}{2} \right)^{-2/3} \right] \left( \frac{M}{M_\odot} \right)^{-1}, \quad (\text{B1})$$

where we normalize the frequency by 100 Hz. Now, we consider the white noise case. We only consider the cosine wave case. These assumptions are sufficient for the purpose here. From Eq. (B1),

$$\frac{\partial f_c}{\partial Q} = 210 \left( \frac{M}{M_\odot} \right)^{-1} Q^{-5/3}. \quad (\text{B2})$$

The metric (A6) in the large  $Q$  limit is derived as

$$ds^2 \sim (0.45Q^{-4/3} - 0.17Q^{-8/3} + 0.13Q^{-2})dQ^2 \\ \sim 0.45Q^{-4/3}dQ^2. \quad (\text{B3})$$

When the maximum loss of the signal to noise ratio  $ds_{\max}^2$  is given, the number of templates needed to achieve this efficiency is estimated as  $N \approx (Q_{\max}^{1/3} - Q_{\min}^{1/3})/ds_{\max}$ . If we consider  $Q_{\min} = 2$  and  $Q_{\max} = 100$ , we only need 20 templates. Thus, the prior knowledge of the black hole mass will make the matched filtering analysis substantially easy.

- 
- [1] LIGO web page: <http://www.ligo.caltech.edu/>
  - [2] VIRGO web page: <http://www.virgo.infn.it/>
  - [3] GEO600 web page: <http://www.geo600.uni-hannover.de/>
  - [4] R. J. Sandeman, in *Second Workshop on Gravitational Wave Data Analysis*, edited by M. Davier and P. Hello (Editions Frontières, Paris, 1998).
  - [5] TAMA300 web page: <http://tamago.mtk.nao.ac.jp/>
  - [6] P. Astone *et al.*, *Phys. Rev. D* **47**, 362 (1993).
  - [7] E. Mauceli *et al.*, *Phys. Rev. D* **54**, 1264 (1996).
  - [8] D.G. Blair *et al.*, *Phys. Rev. Lett.* **74**, 1908 (1995).
  - [9] P. Astone *et al.*, *Astropart. Phys.* **7**, 231 (1997).
  - [10] M. Cerdonio *et al.*, *Class. Quantum Grav.* **14**, 1491 (1997).
  - [11] LISA web page: <http://lisa.jpl.nasa.gov/>
  - [12] E.W. Leaver, *Proc. R. Soc. London* **402**, 285 (1985); *J. Math. Phys.* **27**, 1238 (1986).
  - [13] F. Echeverria, *Phys. Rev. D* **40**, 3194 (1989).
  - [14] L.S. Finn, *Phys. Rev. D* **46**, 5236 (1992).
  - [15] E.E. Flanagan and S.A. Hughes, *Phys. Rev. D* **57**, 4535 (1998); **57**, 4566 (1998).
  - [16] J.D.E. Creighton, *Phys. Rev. D* **60**, 022001 (1999).
  - [17] N. Arnaud *et al.*, *Phys. Rev. D* **67**, 102003 (2003).
  - [18] S.D. Mohanty, *Phys. Rev. D* **57**, 630 (1998).
  - [19] B.J. Owen, *Phys. Rev. D* **53**, 6749 (1996).
  - [20] “TAMA Report 2002 (2nd. ed.)” (in Japanese), edited by K. Tsubono, [ftp://t-munu.phys.s.u-tokyo.ac.jp/pub/TAMA2002/Report\\_V2/main.pdf](ftp://t-munu.phys.s.u-tokyo.ac.jp/pub/TAMA2002/Report_V2/main.pdf)
  - [21] Y. Tsunesada *et al.* (in preparation).
  - [22] Y. Tsunesada and N. Kanda (work in progress).